

LONG MONOTONE PATHS ON SIMPLE 4-POLYTOPES

JULIAN PFEIFLE

ABSTRACT. The *Monotone Upper Bound Problem* (Klee, 1965) asks if the number $M(d, n)$ of vertices in a monotone path along edges of a d -dimensional polytope with n facets can be as large as conceivably possible: Is $M(d, n) = M_{\text{ubt}}(d, n)$, the maximal number of vertices that a d -polytope with n facets can have according to the Upper Bound Theorem?

We show that in dimension $d = 4$, the answer is “yes”, despite the fact that it is “no” if we restrict ourselves to the dual-to-cyclic polytopes. For each $n \geq 5$, we exhibit a realization of a polar-to-neighborly 4-dimensional polytope with n facets and a Hamilton path through its vertices that is monotone with respect to a linear objective function.

This constrasts an earlier result, by which no polar-to-neighborly 6-dimensional polytope with 9 facets admits a monotone Hamilton path.

1. INTRODUCTION

While investigating the complexity of the simplex algorithm for linear programming, Klee [4] in 1965 posed the *Monotone Upper Bound Problem*: For $n > d \geq 2$, he asked for the maximal number $M(d, n)$ of vertices of a d -dimensional polytope with n facets that can lie on a *monotone path*, i.e., on a path along edges that is strictly increasing with respect to a linear objective function.

McMullen’s 1971 *Upper Bound Theorem* [5] (claimed by Motzkin [6] in 1957) states that the maximal number $M_{\text{ubt}}(d, n)$ of vertices that any d -dimensional polytope with n facets can have is achieved by the polars $C_d(n)^\Delta$ of cyclic d -polytopes with n facets.

The Upper Bound Theorem yields, for all $n > d \geq 2$, the inequality

$$(1) \quad M(d, n) \leq M_{\text{ubt}}(d, n),$$

but from this it is not clear whether equality always holds, that is, if for all $n > d \geq 2$ one can construct a simple polar-to-neighborly d -polytope with n facets that admits a monotone Hamilton path with respect to a linear objective function. Equality in (1) is known in the cases $d \leq 3$ and $n \leq d + 2$.

Date: February 16, 2004.

2000 *Mathematics Subject Classification.* 52B12; 52B05.

The author was financed by the DFG Graduiertenkolleg *Combinatorics, Geometry, and Computation* (GRK 588-2), the GIF project *Combinatorics of Polytopes in Euclidean Spaces* (I-624-35.6/1999), and post-doctoral fellowships from MSRI and Institut de Matemàtica de la Universitat de Barcelona.

However, in [7] we show that in fact $M(6, 9) < M_{\text{ubt}}(6, 9)$: there exists *no* realization of the (combinatorially unique) polar-to-neighborly 6-polytope $C_6(9)^\Delta$ with 9 facets and 30 vertices that admits such a monotone Hamilton path.

For the parameters $d = 4$, $n = 8$, one can show using the same (basically combinatorial) methods that there is also no realization of $C_4(8)^\Delta$ with a monotone Hamilton path — but as we will show here, there are other dual-to-neighborly but not dual-to-cyclic 4-dimensional polytopes with 8 facets that admit a realization with a monotone path through all vertices.

In fact, in this paper we prove considerably more: we provide a geometric construction that shows that the inequality (1) is tight in dimension $d = 4$ for all $n \geq 5$.

Main Theorem. *For each integer $m \geq 0$, there exists a simple polar-to-neighborly 4-dimensional polytope Q_m with $n = m + 5$ facets and a linear objective function $f : \mathbb{R}^4 \rightarrow \mathbb{R}$, such that the orientation induced by f on the 1-skeleton of Q_m admits a monotone Hamilton path. Therefore,*

$$M(4, n) = M_{\text{ubt}}(4, n) = \frac{1}{2}n(n - 3).$$

In other words, the maximal number $M(4, n)$ of vertices on a strictly monotone path in the graph of a 4-dimensional polytope with n facets equals the maximal number of vertices that such a polytope can have according to the Upper Bound Theorem.

An interesting feature used in our proof is that for $m \geq 3$, the (polar-to-)neighborly polytopes Q_m are *not* polar to cyclic ones. In fact, exhaustive enumeration shows that already the graph of $C_4(8)^\Delta$ does not satisfy a combinatorial condition necessary for the existence of an monotone path, namely, it does not admit a Hamilton AOF Holt-Klee orientation [2]. This is also true for the graphs of the polytopes $C_4(n)^\Delta$ for $8 \leq n \leq 12$; we conjecture that the graphs of $C_4(n)^\Delta$ for all $n \geq 8$ admit no Hamilton AOF Holt-Klee orientation.

The structure of the paper is as follows: We first give an explicit description, reminiscent of Gale’s Evenness Criterion for polar-to-cyclic polytopes, of the combinatorial structure of a family $\{Q_m^d : d \geq 4 \text{ even}, m \geq 0\}$ of simple (polar-to-)neighborly d -dimensional polytopes with $m + d + 1$ facets (Sections 2 and 3). For $d = 4$, we then use this description to specify a Hamilton path π_m on each $Q_m := Q_m^4$ (Section 4). In Section 5, we start with a monotone path π_0 on a certain realization of the 4-simplex Q_0 , and for $m \geq 0$ inductively realize the polytope Q_{m+1} in such a way that the path π_{m+1} is strictly monotone with respect to a suitable objective function (Theorem 2.5). We proceed in three steps: First, we position Q_m in a suitable way with respect to the standard coordinates on \mathbb{R}^4 (Section 5.4). We then find a “cutting plane” H_{m+1} such that the polytope $Q_m \cap H_{m+1}^{\geq 0}$ has the right combinatorial type (Section 5.5). Finally, we complete the construction in Section 5.6 by applying a projective transformation ψ to \mathbb{R}^4 such that the path $\psi(\pi_m)$ on $Q_{m+1} := \psi(Q_m \cap H_{m+1}^{\geq 0})$ is strictly monotone with respect to the objective function $f : \mathbb{R}^4 \rightarrow \mathbb{R}$, $\mathbf{x} \mapsto x_4$.

2. MAIN RESULTS

Theorem 2.1 (modified Gale’s Evenness Criterion). *For each $m \geq 0$ and even $d \geq 4$, the following sets correspond to the vertices of a combinatorial type \tilde{Q}_m^d of a simple d -dimensional polar-to-neighborly polytope with $n = m + d + 1$ facets.*

▷ Type 1. *The union of one “triplet with a hole” and $d/2 - 1$ pairs of indices*

$$\{j_1, j_1 + 2\} \cup \{j_2, j_2 + 1\} \cup \cdots \cup \{j_{d/2}, j_{d/2} + 1\},$$

where $1 \leq j_1 < n - d + 1$, $j_1 + 3 \leq j_2$, $j_k + 2 \leq j_{k+1}$ for $2 \leq k \leq d/2 - 1$, and $j_{d/2} < n$.

▷ Type 2a. *The union of one triplet, the singleton $\{n\}$, and $d/2 - 2$ pairs of indices*

$$\{j_1, j_1 + 1, j_1 + 2\} \cup \{j_2, j_2 + 1\} \cup \cdots \cup \{j_{d/2-1}, j_{d/2-1} + 1\} \cup \{n\},$$

where $1 \leq j_1 < n - d + 1$, $j_1 + 3 \leq j_2$, $j_k + 2 \leq j_{k+1}$ for $2 \leq k \leq d/2 - 2$, and $j_{d/2-1} < n - 1$.

▷ Type 2b. *The union of $d/2$ pairs of indices*

$$\{1, 2\} \cup \{j_1, j_1 + 1\} \cup \cdots \cup \{j_{d/2-1}, j_{d/2-1} + 1\},$$

where $3 \leq j_1$, $j_k + 2 \leq j_{k+1}$ for $2 \leq k \leq d/2 - 2$, and $j_{d/2-1} < n$.

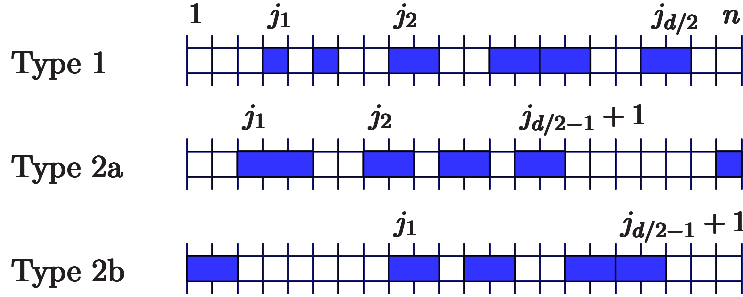


FIGURE 1: The vertex-facet incidences of the polytopes \tilde{Q}_m^d are obtained from these patterns by fixing the dark boxes, and sliding the lighter boxes between 1 and n without overlap. For Type 1, the box $\{i, i + 2\}$ must be regarded as one rigid unit.

Remark 2.2. If we accept for the moment the existence of the polytopes \tilde{Q}_m^d , it is easy to verify that they are polar-to-neighborly by counting the number of vertices using Figure 1:

$$\begin{aligned} f_0(\tilde{Q}_{n-d-1}^d) &= \underbrace{\binom{n-2-(d/2-1)}{d/2}}_{\text{Type 1}} + \underbrace{\binom{n-2-(d/2-2)-1}{d/2-1}}_{\text{Type 2a}} + \underbrace{\binom{n-2-(d/2-1)}{d/2-1}}_{\text{Type 2b}} \\ &= \binom{n-1-d/2}{d/2} + 2 \binom{n-1-d/2}{d/2-1} \\ &= \binom{n-d/2}{d/2} + \binom{n-1-d/2}{d/2-1}, \end{aligned}$$

which is the number of vertices of a simple polar-to-neighborly d -polytope with $n = m+d+1$ facets, since d is assumed even. By [9, Chapter 8], *any* polytope with that many vertices is polar-to-neighborly. \square

From now on, we will always write $\tilde{Q}_m := \tilde{Q}_m^4$.

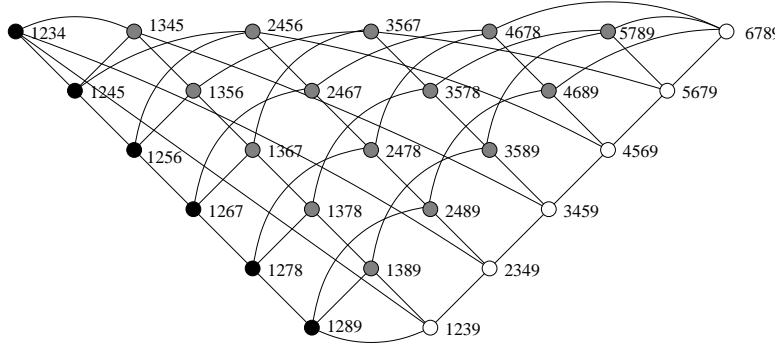


FIGURE 2: Graph of the 4-polytope \tilde{Q}_4 with $n = 9$ facets. Vertices of type 1, 2a, and 2b are drawn in gray, white, and black, respectively. Each vertex is labelled with the facets it is incident to.

Proposition 2.3. Each polytope \tilde{Q}_m admits a Hamilton path $\tilde{\pi}_m$ in its graph that induces an AOF-orientation (cf. Figure 3 and Definition 4.1 below).

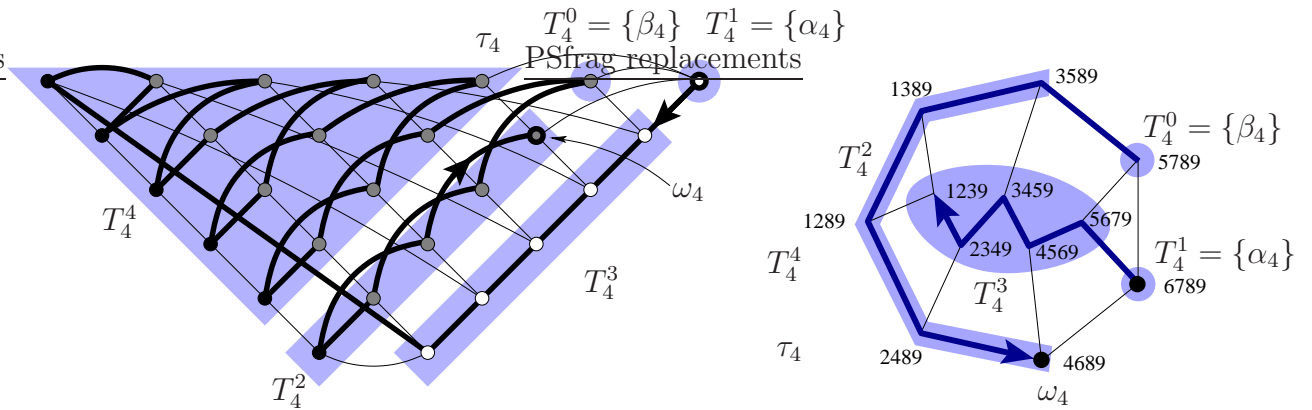


FIGURE 3: *Left:* Graph of \tilde{Q}_4^4 . The partition of the vertices into the tips T^0, T^1, \dots, T^4 is shown, along with the Hamilton path $\tilde{\pi}_4$ (bold). The source α_m is labeled $\{n-3, n-2, n-1, n\}$, and the sink $\omega_m = \{n-5, n-3, n-1, n\}$. See Convention 5.1 for the labels of the other marked vertices. *Right:* The facet F_4^3 with the restriction of $\tilde{\pi}_4$ to it.

Remark 2.4. The crucial property for our realization construction is that the path $\tilde{\pi}_m$ begins in a certain facet F_m^3 of the polytope Q_m (defined below), traverses the rest of Q_m ,

and then returns to F_m^3 (cf. Figure 3). This permits us to add new vertices to the beginning and end of $\tilde{\pi}_m$ by modifying only the facet F_m^3 .

Theorem 2.5. *There exists a family $\{Q_m : m \geq 0\}$ of special realizations of the combinatorial types \tilde{Q}_m , in which each Hamilton path π_m visits the vertices of Q_m in the order given by increasing x_4 -coordinate. This family may be realized inductively starting from the 4-simplex Q_0 in such a way that for all $m \geq 0$, a realization of Q_{m+1} with a monotone Hamilton path π_{m+1} may be obtained from any realization of Q_m with such a path π_m .*

3. CONSTRUCTING THE COMBINATORIAL TYPES \tilde{Q}_m^d

3.1. Facet splitting. We will prove Theorem 2.1 using Barnette's technique of *facet splitting* [1]. Put briefly, for each even $d \geq 4$ we will inductively construct a family $\{(\tilde{Q}_m^d, \mathcal{F}_m) : m \geq 0\}$, where each \tilde{Q}_m^d is the combinatorial type of a simple d -dimensional polytope with $m+d+1$ facets, and \mathcal{F}_m is a flag of faces on \tilde{Q}_m^d (to be defined shortly). We then use \mathcal{F}_m to find a "good" oriented hyperplane H_{m+1} in general position with respect to the vertices of \tilde{Q}_m^d , and set $\tilde{Q}_{m+1}^d := \tilde{Q}_m^d \cap H_{m+1}^{\geq 0}$.

Definition 3.1. Let P be a d -dimensional simple polytope. A *flag of faces* on P is a chain

$$(2) \quad \mathcal{F} : \quad \emptyset = F^{-1} \subset F^0 \subset F^1 \subset \dots \subset F^d = P$$

of faces of P such that $\dim F^i = i$ for $i = 0, 1, \dots, d$. The i -th *tip* of a flag \mathcal{F} is $T^i := \text{vert } F^i \setminus \text{vert } F^{i-1}$, for $0 \leq i \leq d$. We say that the tip T^i is *even* resp. *odd* according to the parity of i . Moreover, for $0 \leq k \leq d$ we set

$$T_{\text{even}}^{\leq k} = \bigcup_{\substack{0 \leq e \leq k \\ e \text{ even}}} T^e \quad \text{and} \quad T_{\text{odd}}^{\leq k} = \bigcup_{\substack{1 \leq o \leq k \\ o \text{ odd}}} T^o.$$

Lemma 3.2. Let P be a simple d -dimensional polytope with n facets, and \mathcal{F} a flag of faces as in (2). Then there exists an affine oriented hyperplane H in general position with respect to P such that $T_{\text{even}}^{\leq d} \subset H^+$ and $T_{\text{odd}}^{\leq d} \subset H^-$. In particular, $P \cap H^{\geq 0}$ is a simple d -polytope with $n+1$ facets.

Proof. Pick an oriented point $\{v\} = H^0 \subset \text{relint } F^1$ such that $T^0 \in (H^0)^+$. Inductively, for $1 \leq k \leq d-1$, if we have already chosen an oriented $(k-1)$ -dimensional affine subspace H^{k-1} in $\text{aff } F^k$ such that

$$(3) \quad T_{\text{even}}^{\leq k} \subset (H^{k-1})^+ \quad \text{and} \quad T_{\text{odd}}^{\leq k} \subset (H^{k-1})^-,$$

we take a k -plane H^k that initially coincides with $\text{aff } F^k$, and orient it in such a way that T^{k+1} lies in $(H^k)^+$ if $k+1$ is even, respectively in $(H^k)^-$ if $k+1$ is odd. Now we rotate H^k by a sufficiently small amount around H^{k-1} in such a way that $T_{\text{even}}^{\leq k} \subset (H^k)^+$. Then (3) even holds with k replaced by $k+1$. By construction, the hyperplane $H := H^{d-1}$ is in general position with respect to P . \square

Definition 3.3. The family $\{(\tilde{Q}_m^d, \mathcal{F}_m) : m \geq 0\}$ of d -dimensional polytopes \tilde{Q}_m^d equipped with flags \mathcal{F}_m of faces is defined in the following way:

(a) \tilde{Q}_0^d is the combinatorial type of the d -simplex $\text{conv}\{v_1, v_2, \dots, v_{d+1}\}$. The flag \mathcal{F}_0 is defined by setting $F_0^i := \text{conv}\{v_1, v_2, \dots, v_{i+1}\}$ for $i = 0, 1, \dots, d$. Then

$$(4) \quad T_0^i := \text{vert}(F_0^i) \setminus \text{vert}(F_0^{i-1}) = \{v_{i+1}\} \quad \text{for } i = 0, 1, \dots, d.$$

(b) For $m \geq 0$, let $H = H_{m+1}$ be the oriented hyperplane given by applying Lemma 3.2 to $P = \tilde{Q}_m^d$ and $\mathcal{F} = \mathcal{F}_m$, and set $\tilde{Q}_{m+1}^d := \tilde{Q}_m^d \cap H_{m+1}^{\geq 0}$ and (cf. Figure 4)

$$T_{m+1}^0 := \text{vert}(\text{conv}(T_m^1 \cup T_m^2) \cap H_{m+1}),$$

$$T_{m+1}^1 := \text{vert}(\text{conv}(T_m^0 \cup T_m^1) \cap H_{m+1}),$$

$$T_{m+1}^j := \text{vert}\left(\text{conv}\left(T_m^{j+1} \cup \bigcup_{\substack{0 \leq k < j \\ k+j=0 \pmod{2}}} T_m^k\right) \cap H_{m+1}\right) \quad \text{for } j = 2, 3, \dots, d-1,$$

$$T_{m+1}^d := \bigcup_{0 \leq k \leq d/2} T_m^{2k}.$$

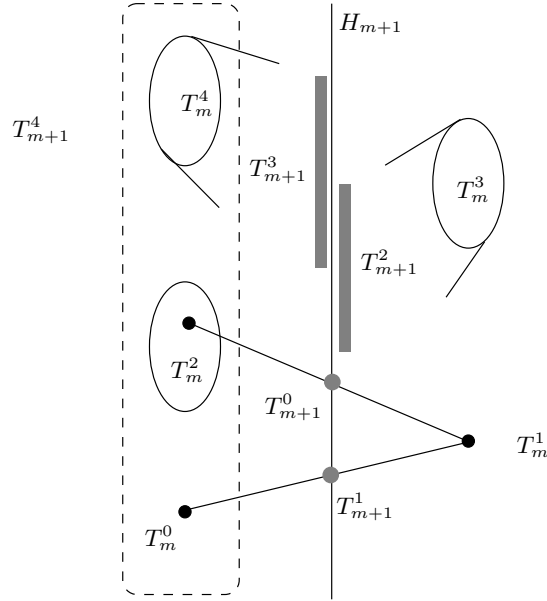


FIGURE 4: New tips in the case $d = 4$.

The flag \mathcal{F}_{m+1} is now defined by $F_{m+1}^j := \bigcup_{i=0}^j T_{m+1}^i$ for $j = 0, 1, \dots, d$. Moreover, put

$$T_{\text{even}}^{\leq k}(m) = \bigcup_{\substack{0 \leq e \leq k \\ e \text{ even}}} T_m^e \quad \text{and} \quad T_{\text{odd}}^{\leq k}(m) = \bigcup_{\substack{1 \leq o \leq k \\ o \text{ odd}}} T_m^o.$$

Remark 3.4.

- (a) The polytopes $C_d(n)^\Delta$ arise by exchanging the definitions of T_{m+1}^0 and T_{m+1}^1 .
- (b) All new vertices arise as the intersection of H_{m+1} with some edge $\text{conv}\{v, w\}$ of \tilde{Q}_m^d , where v and w lie in tips of different parity. Furthermore, all vertices of \tilde{Q}_m^d belonging to even tips are also vertices of \tilde{Q}_{m+1}^d , and vertices in odd tips disappear.

Proposition 3.5. For each $m \geq 0$, the following is true for the pair $(\tilde{Q}_m^d, \mathcal{F}_m)$:

- (a) For all $i, j \in \mathbb{N}$ with $0 \leq i < j \leq d$ and $i + j = 1 \pmod{2}$ and all $v \in T_m^i$, there is exactly one $w \in T_m^j$ such that $\text{conv}\{v, w\} \in \text{sk}^1(\tilde{Q}_m^d)$. This gives rise to bijections $T_{\text{even}}^{\leq k}(m) \cong T_{m+1}^k$ for odd $0 < k < d$ resp. $T_{\text{odd}}^{\leq k}(m) \cong T_{m+1}^k$ for even $0 \leq k \leq d$.
- (b) $|T_m^e| = |T_{m+1}^{e+1}| = \binom{e/2+m}{m}$ for even $e = 0, 2, \dots, d-2$, and $|T_m^d| = \binom{d/2+m}{m}$. This proves again that \tilde{Q}_m^d is polar-to-neighborly.

Proof. (a) This follows because v lies in $F_m^{j-1} = \bigcup_{i=0}^{j-1} T_m^i$, and $\text{conv}(F_m^{j-1})$ is a $(j-1)$ -dimensional face of the simple polytope $\text{conv}(F_m^j) = \text{conv}(F_m^{j-1} \cup T_m^j)$.

(b) We proceed by induction, and can assume that the assertion holds for $m \geq 0$. From the bijections in part (a), we conclude for all even $e = 0, 2, \dots, d-2$ that

$$|T_{m+1}^{e+1}| = |T_{m+1}^e| = \sum_{\substack{i=0 \\ i \text{ even}}}^e |T_m^i| = \sum_{k=0}^{e/2} |T_m^{2k}| = \sum_{k=0}^{e/2} \binom{k+m}{m} = \binom{e/2+m+1}{m+1}.$$

The calculation for $|T_{m+1}^d|$ is similar. The fact that \tilde{Q}_m^d is polar-to-neighborly follows by the same argument as in Remark 2.2, since

$$\begin{aligned} f_0(\tilde{Q}_m^d) &= \sum_{k=0}^{d/2} \binom{k+m}{m} + \sum_{k=0}^{\lfloor (d-1)/2 \rfloor} \binom{k+m}{m} \\ &= \binom{m+d/2+1}{d/2} + \binom{m+\lfloor (d-1)/2 \rfloor+1}{\lfloor (d-1)/2 \rfloor} \\ &= \binom{n-d/2}{d/2} + \binom{n-\lceil (d-1)/2 \rceil-1}{\lfloor (d-1)/2 \rfloor}. \end{aligned}$$

□

3.2. Combinatorics of the family \tilde{Q}_m^d .

Convention 3.6. We introduce labelings to make the combinatorics of the \tilde{Q}_m explicit:

- (a) For any labeling of the facets of a simple d -polytope P with labels in $[n] := \{1, 2, \dots, n\}$, let $\lambda : \text{vert } P \rightarrow \binom{[n]}{d}$ assign to each vertex v of P the set of labels of all facets that v is incident to. We identify a vertex v with its label $\lambda(v)$.
- (b) The facets of the d -simplex \tilde{Q}_0^d on the vertex set $\{v_1, v_2, \dots, v_{d+1}\}$ are labeled in such a way that $v_1 \equiv \lambda(v_1) = [d+1] \setminus \{2\}$, $v_2 = [d+1] \setminus \{1\}$, and $v_j = [d+1] \setminus \{j\}$ for $j = 3, 4, \dots, d+1$ (cf. Figure 5).

(c) The “new” facet $\tilde{Q}_m^d \cap H_{m+1}$ of \tilde{Q}_{m+1}^d is labelled $m + d + 2$.

$$\begin{array}{llll} \{v_5\} = T_0^4 & \text{2b} & 12|34 & \\ \{v_3\} = T_0^2 & \text{2b} & 12|45 & 123|5 \text{ 2a} \quad T_0^3 = \{v_4\} \\ \{v_1\} = T_0^0 & \text{1} & 13|45 & 234|5 \text{ 2a} \quad T_0^1 = \{v_2\} \end{array}$$

FIGURE 5: The labeling of the vertices of the 4-simplex \tilde{Q}_0 according to Convention 3.6(b). Also shown is the classification of the vertices into types 1, 2a, 2b as in Proposition 3.7.

Proposition 3.7. Let $m \geq 0$ and $n = m + d + 1$. A vertex v of \tilde{Q}_m^d lies in T_m^i exactly if

$$\max_n \bar{v} := \max([n] \setminus v) = \begin{cases} m + 2 & \text{for } i = 0, \\ m + 1 & \text{for } i = 1, \\ m + i + 1 & \text{for } 2 \leq i \leq d. \end{cases}$$

Proof. This is true for $m = 0$ by (4) and Convention 3.6, see also Figures 5 and 6. For $m > 0$ and $2 \leq i \leq d - 1$, the statement follows because any vertex $\tilde{v} \in T_m^i$ is of the form $\tilde{v} = \text{conv}\{v, w\} \cap H_m \equiv (v \cap w) \cup \{n\}$ for some $v \in T_{m-1}^k$ and $w \in T_{m-1}^{i+1}$ with $k \leq i$. But then by induction,

$$\max_{n-1} \bar{v} < \max_{n-1} \bar{w} = (m - 1) + (i + 1) + 1 = m + i + 1,$$

so $\max([n] \setminus \tilde{v}) = m + i + 1$ as required. The case $i = d$ follows directly from Definition 3.3, and the cases $i = 0, 1$ are checked similarly. \square

Proof of Theorem 2.1. The existence of the family $\{(\tilde{Q}_m^d, \mathcal{F}_m) : m \geq 0\}$ follows from Lemma 3.2. Using Propositions 3.5 and 3.7, it is somewhat tedious but elementary to verify that for all $m \geq 0$, the vertices of \tilde{Q}_m^d are of the given types. More precisely, all vertices of $T_{\text{even}}^{\leq d}(m)$ are of type 1 or 2b, and $T_{\text{odd}}^{\leq d-1}(m)$ is made up entirely of vertices of type 2a, cf. Figure 6. \square

4. A HAMILTON PATH $\tilde{\pi}_m$ THAT INDUCES AN AOF-ORIENTATION ON \tilde{Q}_m

Definition 4.1. Let P be a simple d -polytope. An acyclic orientation of the graph of P that has a unique sink in each face (including P itself) is called an *AOF-orientation* on P . For any orientation \mathcal{O} of the graph of P and $0 \leq k \leq d$, denote by $h_k(\mathcal{O})$ the number of vertices of in-degree k in \mathcal{O} .

Proposition 4.2. (see e.g. [9, Chap. 8.3] and [3]) An acyclic orientation \mathcal{O} of the graph of a simple d -polytope P is an AOF-orientation if and only if the h -vector of P coincides with the vector $(h_0(\mathcal{O}), h_1(\mathcal{O}), \dots, h_d(\mathcal{O}))$. \square

by $h_k = \binom{n-d-1+k}{k} = \binom{m+k}{k}$ for $k = 0, 1, \dots, d$. Therefore, by Proposition 3.5,

$$\left(|T_m^1|, |T_m^3|, |T_m^4|, |T_m^2|, |T_m^0|\right) = (h_0, h_1, h_2, h_3, h_4).$$

By Proposition 4.2, it suffices to verify using Figure 3 that if the orientation of each edge of the graph of \tilde{Q}_m is consistent with the total ordering induced by $\tilde{\pi}_m$, then the vertices of T^1 , T^3 , resp. T^4 all have in-degree 0, 1 resp. 2, furthermore T^0 and all but one of the vertices of T^2 have in-degree 3, and this vertex, the sink, has in-degree 4. \square

5. REALIZING THE MONOTONE HAMILTON PATHS

In this section we prove Theorem 2.5, and therefore our Main Theorem.

5.1. Outline of the inductive construction. For all $m \geq 0$, we first find an oriented hyperplane H_{m+1} that separates the *odd part* $T_{\text{odd}}^{\leq 4}(m) = T_m^1 \cup T_m^3$ from the *even part* $T_{\text{even}}^{\leq 4}(m) = T_m^0 \cup T_m^2 \cup T_m^4$ of π_m . We then create an intermediate pair $(Q'_{m+1}, \mathcal{F}'_{m+1})$ as in Proposition 3.5: $Q'_{m+1} := Q_m \cap H_{m+1}^{\geq 0}$ is a simple polar-to-neighborly polytope of the same combinatorial type as \tilde{Q}_{m+1} , and the flag \mathcal{F}'_{m+1} of faces is defined as in Definition 3.3(b).

Our combinatorial model \tilde{Q}_{m+1} provides us with a Hamilton path π_{m+1} on Q'_{m+1} that is not yet monotone with respect to the objective function $f : \mathbf{x} \mapsto x_4$. However, we will choose H_{m+1} in such a way that there exists a pencil

$$\mathcal{H} = \{H_t : t \in \mathbb{P}^1(\mathbb{R}) \cong \mathbb{R} \cup \{\infty\}\}$$

of hyperplanes in \mathbb{R}^4 with the following properties:

- (S1) The common intersection of all hyperplanes in \mathcal{H} is a 2-flat $R = \bigcap_{t \in \mathbb{P}^1(\mathbb{R})} H_t$ (the *axis* of \mathcal{H}), and $\text{vert } Q'_{m+1} \cap R = \emptyset$.
- (S2) The pencil \mathcal{H} “sorts the vertices of Q'_{m+1} correctly”: If $p \in H_r$ and $q \in H_s$ are vertices of Q'_{m+1} with $r, s \neq \infty$ and p precedes q in π_{m+1} , then $r < s$.

We then apply a projective transformation ψ to $\mathbb{R}^4 \subset \mathbb{P}^4(\mathbb{R})$ that maps H_∞ to the hyperplane at infinity. Because the common intersection R of all hyperplanes in \mathcal{H} is also mapped to infinity, the image $\psi(\mathcal{H}^b) = \psi(\mathcal{H} \setminus H_\infty) = \{\psi(H_t) : t \in \mathbb{R}\}$ is a family of parallel affine hyperplanes in \mathbb{R}^4 . The new objective function f is then defined by the common normal vector to the hyperplanes in $\psi(\mathcal{H}^b)$, and the Hamilton path $\psi(\pi_{m+1})$ on $Q_{m+1} := \psi(Q'_{m+1})$ is strictly monotone with respect to f_{m+1} by (S2).

5.2. Properties of the family of polytopes.

Notation 5.1. We use the following names for some special vertices of \tilde{Q}_m :

- ▷ The source $\{\alpha_m\} = \{n-3, n-2, n-1, n\}$ of $\tilde{\pi}_m$ is called α_m (so that $T_m^1 = \{\alpha_m\}$).
- ▷ The sink is $\omega_m := \{n-5, n-3, n-1, n\} \in T_m^2$.
- ▷ $\beta_m := \{n-4, n-2, n-1, n\}$ (so that $T_m^0 = \{\beta_m\}$).
- ▷ $\tau_m := \{n-5, n-3, n-2, n-1\} \in T_m^4$.

Proposition 5.2.

- (a) The induced subgraph of $sk^1(Q_m)$ on $T_m^1 \cup T_m^3$ is a path of length $m + 1$ on the $m + 2$ vertices $v_0^m = \alpha_m, v_1^m, \dots, v_{m+1}^m$, and the induced subgraph on T_m^2 is a path $w_1^m, w_2^m, \dots, w_{m+1}^m$.
- (b) For $0 \leq i \leq m$, the edge $e_i = \text{conv}\{v_i^m, v_{i+1}^m\}$ in T_m^3 is incident to a 2-face G_i of Q_m such that the vertices of $G_i \setminus e_i$ are consecutive in $\pi_m \cap T_m^4$.
- (c) For $1 \leq i \leq m$, the edge f_i of Q_m that connects w_i^m and w_{i+1}^m in $T_m^2 \cap \pi_m$ is incident to a quadrilateral R_i whose other two vertices are consecutive in $T_m^4 \cap \pi_m$.
- (d) Set $G(m) = \text{vert} \bigcup_{i=0}^m G_i \setminus e_i$ and $R(m) = \text{vert} \bigcup_{i=1}^m R_i \setminus f_i$. Then $G(m) \cup R(m) = T_m^4$, and $G(m) \cap R(m) = \tau_m$.

Proof. (a) All vertices of T_m^3 are of the form $\{i, i + 1, i + 2, n\}$ for $1 \leq i \leq n - 3$, and the only way for two such vertices v_i^m and v_j^m to be adjacent for $i < j$ is to have $j = i + 1$. The statement about the w_i^m follows in a similar way. (b) For $1 \leq i \leq m + 1$, the 2-face incident to $v_{m+2-i} = \{i, i + 1, i + 2, n\}$ and $v_{m+1-i} = \{i + 1, i + 2, i + 3, n\}$ that is the intersection of the facets $i + 1$ and $i + 2$ consists of the vertices of Figure 8. The claim (b) follows because these vertices form a contiguous segment of π_m , and (c) and (d) from Figure 9 (left). \square

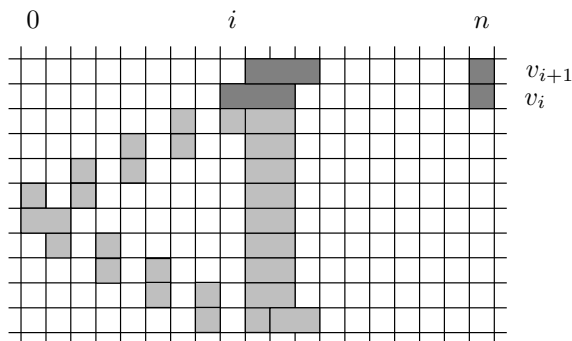


FIGURE 8: Vertices of a 2-face incident to $v_i = \{i, i + 1, i + 2, n\}$ and $v_{i+1} = \{i + 1, i + 2, i + 3, n\}$ (dark) in $T_m^1 \cup T_m^3$. The light vertices lie in T_m^4 and form a subpath of π_m .

Observation 5.3. The new start vertex α_{m+1} of $\tilde{\pi}_{m+1}$ lies on $\text{conv}\{\alpha_m, \beta_m\}$, the new end vertex ω_{m+1} on $\text{conv}\{v_1^m, \beta_m\}$, and β_{m+1} on $\text{conv}\{\alpha_m, \omega_m\}$; see Figure 9 (right).

5.3. Start of the induction and inductive invariant. We work in \mathbb{R}^4 with standard coordinate vectors e_1, e_2, e_3, e_4 . An essential tool will be *shear transformations*: these are linear maps $\sigma_{i,j}^a : \mathbb{R}^4 \rightarrow \mathbb{R}^4$ for $i, j \in \{1, 2, 3, 4\}, i \neq j$, and $a \in \mathbb{R}$ whose matrix is $I_4 + a\delta_{i,j}$ with respect to the standard basis of \mathbb{R}^4 . Here I_4 is the 4×4 unit matrix and $\delta_{i,j}$ is the 4×4 matrix whose only nonzero entry is a 1 in position (i, j) . In particular, $\sigma_{i,j}^a$ maps e_i to $e_i + ae_j$, and the standard basis vectors $e_k, k \neq i$, to themselves.

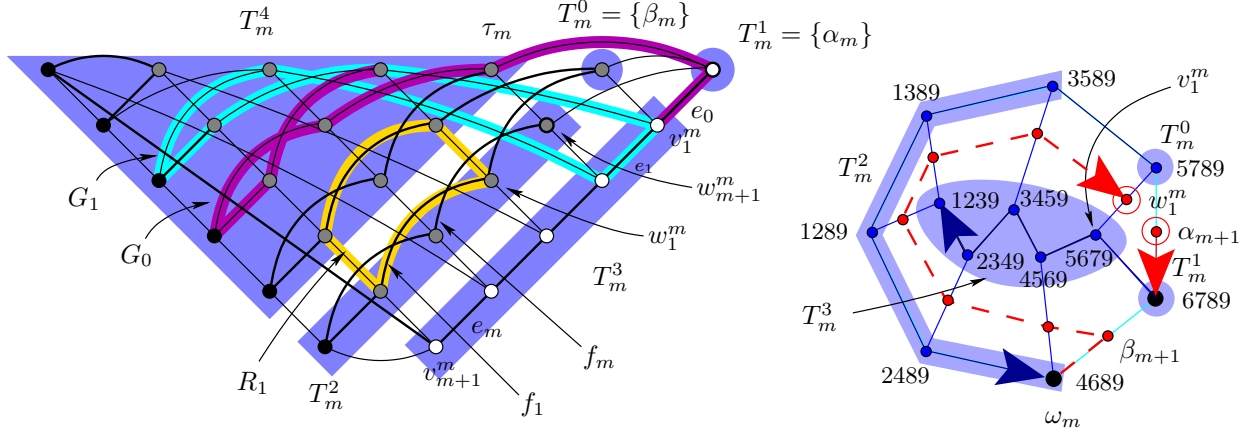


FIGURE 9: *Left:* More details about the graph of Q_m . We have highlighted the graphs of the 2-faces G_0 and G_1 that correspond to the edges e_0 and e_1 by Proposition 5.2 (b), and the 2-face R_1 that corresponds to the edge f_1 according to Proposition 5.2 (c). *Right:* The portion of the new Hamilton path $\tilde{\pi}_{m+1}$ in the facet F_m^3 .

The start of the induction is the pair (Q_0, \mathcal{F}_0) , where Q_0 is the 4-simplex whose vertices v_1, v_2, v_3, v_4, v_5 are given by the columns of the matrix

$$(5) \quad \begin{pmatrix} 0 & 0 & 1 & 0 & 0 \\ 0 & 1 & 0 & 0 & 0 \\ -3 & -1 & 3 & 2 & 1 \\ -2 & -1/2 & 0 & 1/4 & 2 \end{pmatrix},$$

and \mathcal{F} is the flag $\mathcal{F}_0 : F_0^0 \subset F_0^1 \subset \dots \subset F_0^4 = Q_0^4$ of faces labeled as in Definition 3.3. In particular, the vertices v_i lie in the following tips,

$$\begin{array}{c|c|c|c|c} v_1 & v_2 & v_3 & v_4 & v_5 \\ \hline T_0^1 & T_0^3 & T_0^4 & T_0^0 & T_0^2 \end{array},$$

$F_0^2 = \text{conv}\{v_1, v_4, v_5\}$, $F_0^3 = \text{conv}\{v_1, v_2, v_4, v_5\}$, and $\pi_0 = (v_1, v_2, v_3, v_4, v_5)$.

For all $m \geq 0$ the polytopes Q_m will maintain the following property:

(M1) The Hamilton path π_m in the 1-skeleton of Q_m is strictly monotone with respect to the objective function $f : \mathbb{R}^4 \rightarrow \mathbb{R}$, $\mathbf{x} \mapsto x_4$.

5.4. Induction step I: Positioning the polytope. In this and the following section, we will position the polytope Q_m in such a way that the coordinate subspaces of \mathbb{R}^4 are compatible with the flag \mathcal{F}_m . More precisely,

- ▷ $F_m^3 = Q_m \cap \{\mathbf{x} \in \mathbb{R}^4 : x_1 = 0\}$, and $T_m^4 \subset \{\mathbf{x} \in \mathbb{R}^4 : x_1 > 0\}$; and
- ▷ the hyperplane $H_S = \{\mathbf{x} \in \mathbb{R}^4 : x_3 = 0\}$ will separate $T_{\text{even}}^{\leq 4}(m)$ from $T_{\text{odd}}^{\leq 4}(m)$.

Lemma 5.4. Let π be the linear projection $\pi : \mathbb{R}^4 \rightarrow \mathbb{R}\langle e_3, e_4 \rangle$, and use the notation of Convention 5.1 and Proposition 5.2(a). Then there exists a non-singular affine transformation σ of \mathbb{R}^4 such that $Q_m \equiv \sigma(Q_m)$ satisfies the following additional conditions, while $\pi_m \equiv \sigma(\pi_m)$ still satisfies (M1):

- (M2) $F_m^2 \subset \{\mathbf{x} \in \mathbb{R}^4 : x_1 = 0\}$.
- (M3) $\text{aff } F_m^3 = \{\mathbf{x} \in \mathbb{R}^4 : x_1 = 0\}$ and $Q_m \subset \{\mathbf{x} \in \mathbb{R}^4 : x_1 \geq 0\}$.
- (M4) $(\alpha_m)_2 = 0$, $r_2 < 0$ for all $r \in F_m^2 \setminus \{\alpha_m\}$, and $(\beta_m)_2 < (v_1^m)_2$.
- (M5) The image of F_m^2 under π is full-dimensional: $\dim \text{aff}(\pi(F_m^2)) = 2$.
- (M6) The 3-flat $H_S = \{\mathbf{x} \in \mathbb{R}^4 : x_3 = 0\}$ strictly separates $T_{\text{even}}^{\leq 4}(m)$ from $T_{\text{odd}}^{\leq 4}(m)$.
Moreover, we may choose the point of $H_S \cap F_m^3$ of lowest 4-coordinate to be $\alpha_{m+1} = \text{conv}\{\alpha_m, \beta_m\} \cap H_S$, where $(\alpha_{m+1})_4 = \tau_4 := (\tau_m)_4$.

Proof. Properties (M2) and (M3) are a matter of trivial affine transforms that can be chosen to leave the 4-coordinates invariant, thereby maintaining (M1), and property (M4) can be achieved via a translation and a shear $\sigma_{2,4}^a : x_2 \mapsto x_2 + ax_4$.

For (M5), choose $t \in F_m^2$ with $t_4 = q_4$ for some $q \in T_m^3$; such a point exists, since $\alpha_m \in F_m^2$, and $(\alpha_m)_4 < q'_4 < \max\{s_4 : s \in F_m^2\}$ for all $q' \in T_m^3$ by (M1) and Remark 2.4. Translate t such that $t = (0, t_2, 0, 0)$ with $t_2 < 0$, and apply a shear transform $\sigma_{3,2}^b : x_3 \mapsto x_3 + bx_2$ to \mathbb{R}^4 , where $b \in \mathbb{R}$ is chosen such that $\pi(\sigma_{3,2}^b(q)) = \pi(\sigma_{3,2}^b(t))$. This can be done because $\pi(t) - \pi(q) \in \mathbb{R}\pi(e_3)$. Then (M5) is fulfilled because $\dim \text{aff } F_m^3 = 3$: supposing that $\dim \text{aff}(\pi(F_m^2)) = 1$ would imply via $t \in F_m^2$ and $q \in F_m^3$ that $q \in \text{aff } F_m^2$; however, this is absurd by the choice $q \in T_m^3$. Note that none of the maps we used affects (M2)–(M4).

For (M6), define \tilde{b} to be the point of greatest 3-coordinate of $F_m^2 \cap \{\mathbf{x} \in \mathbb{R}^4 : x_4 = \tau_4\}$. In particular, $\tilde{b}_4 > \max_{z \in T^3} z_4$ by (M1), and \tilde{b} lies either on the edge $\text{conv}\{\alpha_m, \beta_m\}$ or on the edge $\text{conv}\{\alpha_m, \omega_m\}$ of $F_m^2 \subset Q_m$ (cf. Figure 10).

Possibly using the transform $x_3 \mapsto -x_3$, we can achieve $\tilde{b} \in \text{conv}\{\alpha_m, \beta_m\}$, and $\tilde{b} = \alpha_{m+1}$ after a translation along the 3-axis. Now choose a non-horizontal line ℓ through α_{m+1} such that $\pi(\ell)$ separates $\pi(T_m^1 \cup T_m^3)$ from $\pi(F_m^2 \setminus T_m^1)$ (for example, perturb $\ell = \alpha_{m+1} + \mathbb{R}e_3$), translate Q_m again such that $\alpha_{m+1} = 0$, and apply a shear $\sigma_{3,4}^c : x_3 \mapsto x_3 + cx_4$ to \mathbb{R}^4 such that $\ell' := \sigma_{3,4}^c(\ell) = \{\mathbf{x} \in \mathbb{R}^4 : x_1 = x_3 = 0\} \cap \text{aff } F_m^2$ is vertical, and $x_3 < 0 < y_3$ for all $x \in T_m^1 \cup T_m^3$ and $y \in F_m^2 \setminus T_m^1$ (cf. Figure 10). If the hyperplane $\pi^{-1}(\pi(\ell'))$ does not yet separate T_m^1 from T_m^4 , apply another shear $\sigma_{3,1}^d : x_3 \mapsto x_3 + dx_1$ with $d > 0$ until it does (note that (M3) already holds), and then define $H_S := \pi^{-1}(\pi(\ell'))$. This hyperplane then separates the odd and even parts of π_m by construction, and $(\alpha_{m+1})_4 = \tau_4$ also by construction and because the shears $\sigma_{3,4}^c$ and $\sigma_{3,1}^d$ do not affect 4-coordinates. Neither do they affect conditions (M1)–(M5), so we define σ as the composition of all these maps. \square

Remark 5.5. The conditions (M1)–(M6) are satisfied by the coordinates (5) for Q_0 .

5.5. Induction step II: Finding the cutting plane. In this section, we will find a hyperplane H_{m+1} that gives rise to a polytope $Q'_{m+1} = Q_m \cap H_{m+1}^{\geq 0}$ of the same combinatorial

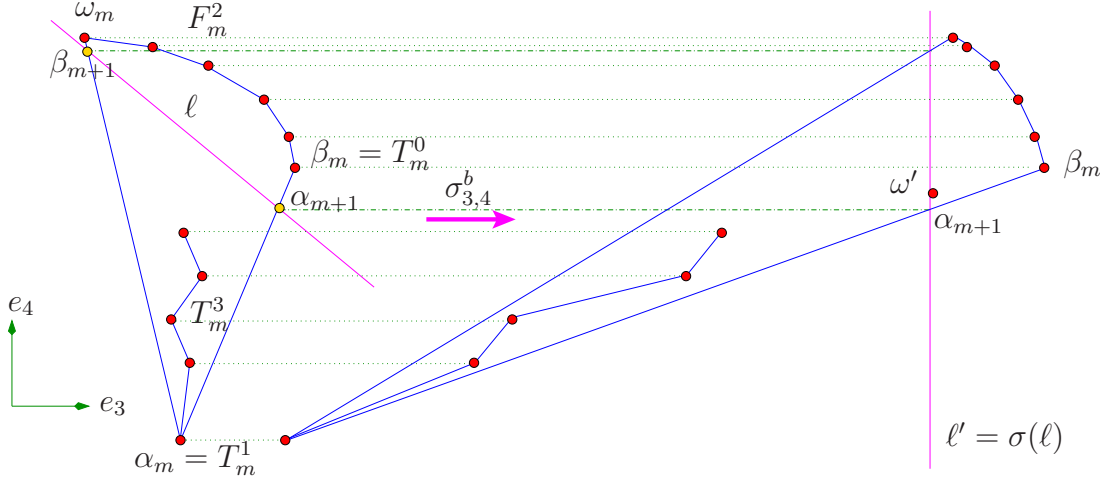


FIGURE 10: Positioning the polytope, step (M6). The map $\sigma_{3,4}^b$ shears the polytope until (the preimage under π of) a vertical line ℓ' separates the odd from the even tips. On the right, the approximate position of ω' is marked; cf. Lemma 5.7.

type as \tilde{Q}_{m+1} . Namely, assume that (M1)–(M6) hold, define H_{m+1} to be the hyperplane $\{\mathbf{x} \in \mathbb{R}^4 : \mathbf{n}^T \mathbf{x} = 0\}$ with $\mathbf{n} = (0, -\delta, 1, \varepsilon)^T$ for some small $\varepsilon \gg \delta > 0$, and assign the label $n + 1 = m + d + 2$ to H_{m+1} . Note that H_{m+1} converges to H_S as $\varepsilon, \delta \rightarrow 0$.

Remark 5.6. Up to now, we have put the facet F_m^3 into the 3-plane $\{\mathbf{x} \in \mathbb{R}^4 : x_1 = 0\}$ and the tip T^4 into the half-space $\{\mathbf{x} \in \mathbb{R}^4 : x_1 > 0\}$. This allows us to move “almost all” of the vertices of π_m (namely, the portion inside T_m^4) “out of the way”, via a shear $\sigma_{3,1}^a$ that only affects 3-coordinates. These “old” vertices will be dealt with in Lemma 5.8 below.

We still need to arrange for the first and last part of π_{m+1} to be traversed in the right order. We achieve this by adjusting the position of H_{m+1} via the parameters ε and δ in the definition of \mathbf{n} (note that we chose $n_1 = 0$, because we are already done with T_m^4). If $\delta = 0$, then $\pi(H_{m+1})$ is a line whose slope is determined by ε . We choose $\varepsilon > 0$ to ‘push out’ the first part $T_{m+1}^1 \cup T_{m+1}^3$ of the new path π_{m+1} . However, if we left $\delta = 0$ we would not correctly sweep the last portion $T_{m+1}^0 \cup T_{m+1}^2$. Items (M8)–(M10) of Lemma 5.7 guarantee a correct sweep in Lemma 5.8 for sufficiently small $0 < \delta \ll \varepsilon$.

Lemma 5.7. Assume conditions (M1)–(M6) and $(\alpha_{m+1})_3 = (\alpha_{m+1})_4 = 0$, and fix vertices $q \in T_{\text{odd}}^{\leq 4}(m)$ and $s \in T_{\text{even}}^{\leq 4}(m)$. Let $q' = \text{conv}\{q, s\} \cap H_{m+1}$ be the intersection with H_{m+1} of the line through q and s (which is not necessarily an edge of Q_m). Then, if $a > 0$ is sufficiently large and $0 < \delta \ll \varepsilon$ are sufficiently small, the image $\sigma_{3,1}^a(Q_m)$ of Q_m under the shear $\sigma_{3,1}^a$ satisfies the following conditions (M7)–(M10); cf. also Figure 12 below.

- (M7) $q'_3 > 0$ for $0 < \delta \ll \varepsilon$, and $q'_3 \searrow 0$ as $\delta, \varepsilon \searrow 0$. In other words, all points in $\sigma_{3,1}^a(Q_m) \cap H_{m+1}$ can be chosen to have positive 3-coordinate, but to lie arbitrarily close to H_S .

- (M8) Set $u := (v_1^{m+1})' = \text{conv}\{\alpha_m, \tau_m\} \cap H_{m+1}$ and suppose that $q' \neq u$. Then the image $\pi(\text{aff}\{u, q'\}) \subset \mathbb{R}\langle e_3, e_4 \rangle$ of the line through u and q' under π comes arbitrarily close to being vertical as $a \rightarrow \infty$ and $\varepsilon, \delta \rightarrow 0$.
- (M9) Set $\alpha' := \alpha'_{m+1} = \text{conv}\{\alpha_m, \beta_m\} \cap H_{m+1}$. If $q, \bar{q} \in T_m^3$ and $q_4 < \bar{q}_4$, so that $q', \bar{q}' \in T_{m+1}^3$ and $q'_4 < \bar{q}'_4$, then the slope $\sigma_{\alpha' \bar{q}'}$ of the line $\pi(\text{aff}\{\alpha', \bar{q}'\})$ is greater than the slope $\sigma_{\alpha' q'}$ of the line $\pi(\text{aff}\{\alpha', q'\})$ (and both are negative).
- (M10) Set $\omega' := \omega'_{m+1} = \text{conv}\{\beta_m, v_1^m\} \cap H_{m+1}$. Then the slope $\sigma_{\omega' \alpha'}$ of $\pi(\text{aff}\{\omega', \alpha'\})$ is less than the slope $\sigma_{\omega' u}$ of $\pi(\text{aff}\{\omega', u\})$.

Proof. We abbreviate $\sigma = \sigma_{3,1}^a$. For (M7), we have $\text{conv}\{q, s\} \cap H_{m+1} \neq \emptyset$ since q and s are separated by H_{m+1} for small enough δ, ε . We calculate the intersection point $q' = \text{conv}\{q, s\} \cap H_{m+1}$ by solving $\mathbf{n}^T \mathbf{q} + \mu \mathbf{n}^T (\mathbf{s} - \mathbf{q}) = 0$ for μ , obtaining

$$\mathbf{q}' = \mathbf{q} + \frac{\mathbf{n}^T \mathbf{q}}{\mathbf{n}^T (\mathbf{q} - \mathbf{s})} (\mathbf{s} - \mathbf{q}).$$

By (M2), the map σ leaves the points α', q , and ω' invariant, and maps \mathbf{s} to $\sigma(\mathbf{s}) = \mathbf{s} + a s_1 \mathbf{e}_3$; as a consequence, $\mathbf{n}^T \sigma(\mathbf{s}) = \mathbf{n}^T \mathbf{s} + a s_1$. Using $\mathbf{n}^T \mathbf{q} = -\delta q_2 + q_3 + \varepsilon q_4$, we obtain

$$\begin{aligned} \sigma(\mathbf{q}') &= \mathbf{q} + \frac{\mathbf{n}^T \mathbf{q}}{\mathbf{n}^T (\mathbf{q} - \mathbf{s}) - a s_1} (\mathbf{s} - \mathbf{q} + a s_1 \mathbf{e}_3) \\ (6) \quad &\xrightarrow{a \rightarrow \infty} \mathbf{q} + (0, 0, -\mathbf{n}^T \mathbf{q}, 0)^T = (0, q_2, \delta q_2 - \varepsilon q_4, q_4)^T. \end{aligned}$$

Because $q_4 < (\alpha_{m+1})_4 = 0$, we can choose $0 < \delta \ll \varepsilon$ so small that $\sigma(\mathbf{q}')_3 > 0$ (note that $q_2 \leq 0$ by (M4)). In particular, we obtain $\sigma(\mathbf{q}')_3 \searrow 0$ as $\varepsilon, \delta \searrow 0$.

Statement (M8) follows from (6) and the fact that

$$\lim_{a \rightarrow \infty} \frac{\sigma(\mathbf{q}')_4 - \sigma(\mathbf{u})_4}{\sigma(\mathbf{q}')_3 - \sigma(\mathbf{u})_3} = \frac{q_4 - u_4}{\delta(q_2 - u_2) - \varepsilon(q_4 - u_4)}.$$

For (M9), note that since α' is invariant under σ ,

$$\sigma_{\alpha' q'} = \frac{\sigma(\mathbf{q}')_4 - \alpha'_4}{\sigma(\mathbf{q}')_3 - \alpha'_3} \xrightarrow{a \rightarrow \infty} \frac{q_4 - \alpha'_4}{\delta q_2 - \alpha'_3 - \varepsilon q_4},$$

and similarly for \bar{q} ; the statement now follows from $q_4 < \bar{q}_4$ and $0 < \delta \ll \varepsilon$.

To prove (M10), set $\alpha := \alpha_m$, $\beta := \beta_m$, $v := v_1^m$ and $\tau := \tau_m$. Then $u = \text{conv}\{\alpha, \tau\} \cap H_{m+1}$, $\alpha' = \text{conv}\{\alpha, \beta\} \cap H_{m+1}$, and $\omega' = \text{conv}\{v, \beta\} \cap H_{m+1}$. We need to verify that

$$\sigma_{\omega' \alpha'} := \frac{\alpha'_4 - \omega'_4}{\alpha'_3 - \omega'_3} < \frac{u_4 - \omega'_4}{u_3 - \omega'_3} =: \sigma_{\omega' u}.$$

From equation (6) and condition (M4), we deduce that $\lim_{a \rightarrow \infty} u = (0, 0, -\varepsilon\alpha_4, \alpha_4)^T$. For α' and ω' we get the following expressions:

$$\alpha' = \alpha + \frac{\mathbf{n}^T \alpha}{\mathbf{n}^T (\alpha - \beta)} (\beta - \alpha) = \begin{pmatrix} 0 \\ 0 \\ \alpha_3 \\ \alpha_4 \end{pmatrix} + \frac{\alpha_3 + \varepsilon\alpha_4}{\delta\beta_2 + \alpha_3 - \beta_3 + \varepsilon(\alpha_4 - \beta_4)} \begin{pmatrix} 0 \\ \beta_2 \\ \beta_3 - \alpha_3 \\ \beta_4 - \alpha_4 \end{pmatrix},$$

$$\omega' = \mathbf{v} + \frac{\mathbf{n}^T \mathbf{v}}{\mathbf{n}^T (\mathbf{v} - \beta)} (\beta - \mathbf{v}) = \begin{pmatrix} 0 \\ v_2 \\ v_3 \\ v_4 \end{pmatrix} + \frac{-\delta v_2 + v_3 + \varepsilon v_4}{-\delta(v_2 - \beta_2) + v_3 - \beta_3 + \varepsilon(v_4 - \beta_4)} \begin{pmatrix} 0 \\ \beta_2 - v_2 \\ \beta_3 - v_3 \\ \beta_4 - v_4 \end{pmatrix}.$$

For convenience, we will verify that $1/\sigma_{\omega'\alpha'} > 1/\sigma_{\omega'u}$. Indeed, expanding these expressions in terms of δ, ε , we obtain

$$\frac{1}{\sigma_{\omega'\alpha'}} = \frac{\beta_3 v_2 - \beta_2 v_3 + \overbrace{\alpha_3(\beta_2 - v_2)}^{t_1}}{v_3(\alpha_4 - \beta_4) + \beta_3(v_4 - \alpha_4) + \underbrace{\alpha_3(\beta_4 - v_4)}_{t_2}} \delta - \varepsilon + p_1(\delta, \varepsilon),$$

$$\frac{1}{\sigma_{\omega'u}} = \frac{\beta_3 v_2 - \beta_2 v_3}{v_3(\alpha_4 - \beta_4) + \beta_3(v_4 - \alpha_4)} \delta - \varepsilon + p_2(\delta, \varepsilon),$$

where p_1 and p_2 are power series in δ, ε with min-degree at least 2. Notice that up to terms of degree at least 2 in δ, ε , the two formulas are equal except for the expressions t_1 resp. t_2 in the numerator resp. denominator of $1/\sigma_{\omega'\alpha'}$. Therefore, we can write the difference between the inverses of the slopes as

$$\frac{1}{\sigma_{\omega'\alpha'}} - \frac{1}{\sigma_{\omega'u}} = \left(\frac{A + t_1}{B + t_2} - \frac{A}{B} \right) \delta + p_3(\delta, \varepsilon).$$

Since $\alpha_3 < (\alpha_{m+1})_3 < 0$ by assumption and $\beta_2 < v_2$ by (M4), we obtain $t_1 > 0$; and the inductive assumption (M1) implies that $\beta_4 > v_4$ and therefore $t_2 < 0$. The claim follows. \square

5.6. Induction step III: The projective transformation. Finally, we construct a 1-parameter family $\mathcal{H} = \{H_t : t \in \mathbb{P}^1(\mathbb{R})\}$ of hyperplanes that contains a 2-plane R as their common ‘‘axis’’, as in Section 5.1. Let $O = \pi(b + \varepsilon_1(\omega - \alpha) - \varepsilon_3 e_3)$ for some small $\varepsilon_1, \varepsilon_3 > 0$, so that O lies outside but very close to the edge $\text{conv}\{\alpha, \omega\}$ of $\pi(F_{m+1}^2)$, and define the 2-plane $R \subset \mathbb{R}^4$ to be $R = \pi^{-1}(O)$.

Lemma 5.8. Let \mathcal{H} be the pencil of hyperplanes in \mathbb{R}^4 sharing the 2-plane R , and such that $\pi(H_\infty)$ is the line through O parallel to $\text{conv}\{\alpha, \omega\}$, and the slope of $\pi(H_r)$ is smaller than the slope of $\pi(H_s)$ exactly if $r < s$. Then \mathcal{H} fulfills (S2), i.e., it sorts the vertices of Q_{m+1} in the order given by π_{m+1} .

Proof. We examine the pieces of π_{m+1} in order; cf. Figure 12.

- ▷ $T_{m+1}^1 = \{\alpha\}$ is the start of π_{m+1} : This follows for small enough ε_3 by (M10).
- ▷ T_{m+1}^3 is traversed next, in the right order, and before T_{m+1}^4 : The first two statements follow from (M7), (M8) and (M9), and the last one because $z_3 \rightarrow \infty$ as $a \rightarrow \infty$ for any $z \in T_m^4$, while the 3-coordinates of T_{m+1}^3 remain bounded by (M7).
- ▷ The correct order in $T_m^4 \subset T_{m+1}^4$. By Proposition 5.2(b), each of the edges $e_i = \text{conv}\{v_i^m, v_{i+1}^m\}$, $0 \leq i \leq m$, of $T_m^1 \cup T_m^3$ is incident to an $(m+1)$ -gonal 2-face G_i (see Figure 9), and the edges E_i of G_i not incident to e_i form a monotone subpath of π_{m+1} . This implies that for each $e_i \in T_m^3$, the slopes of the projection of each E_i to $\mathbb{R}\langle e_3, e_4 \rangle$ are strictly positive (and, by convexity, monotonically decreasing; see Figure 11).

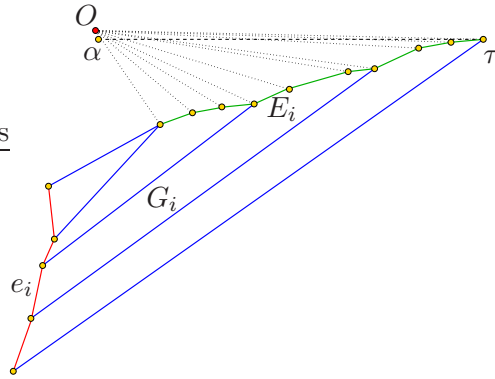


FIGURE 11: Convexity of the $(m+1)$ -gonal faces enforces the correct order in $T_m^4 \subset T_{m+1}^4$.

Therefore, $\pi(\bigcup_{i=0}^m E_i)$ is a strictly increasing chain of edges, and this remains true after applying the linear map $\sigma = \sigma_{3,1}^a$ by invariance of the e_i 's and all 4-coordinates under σ , and the convexity of the projections of 2-faces. The correct order up to τ in $T_m^4 \subset T_{m+1}^4$ follows from condition (M6): $\alpha_4 \geq s_4$ for all $s \in \bigcup_{i=0}^m \text{vert } G_i \setminus \text{vert } e_i$. Similarly, the 4-gonal 2-faces incident to T_m^2 of Proposition 5.2(c) enforce the right order between τ and T_m^0 .

- ▷ T_{m+1}^2 is traversed after T_{m+1}^4 : Since β , the first vertex of π_{m+1} to come after T_{m+1}^4 , lies on $\text{conv}\{\alpha_m, \omega_m\}$, this can be achieved by choosing ε and ε_1 suitably small.
- ▷ Correct order in T_{m+1}^2 and T_{m+1}^0 . This follows because the convex polygon $\pi(F_{m+1}^2)$ is star-shaped with respect to any point on its boundary, and the choice of O close to an edge of $\pi(F_{m+1}^2)$.

This concludes the proof of Lemma 5.8. \square

Finally, we apply the projective transform $\psi : \mathbb{R}^4 \rightarrow \mathbb{R}^4$, $\mathbf{x} \mapsto \mathbf{x}/(\mathbf{a}\mathbf{x} - a_0)$ that sends the 3-plane $H_\infty = \{\mathbf{x} \in \mathbb{R}^4 : \mathbf{a}\mathbf{x} = a_0\}$ to infinity, and set $Q_{m+1} := \psi(Q'_{m+1})$. Lemma 5.8 then implies the inductive condition (M1), namely that Q_{m+1} admits an monotone Hamilton path π_{m+1} . The proof of Theorem 2.5, and so of the Main Theorem, is concluded. \square

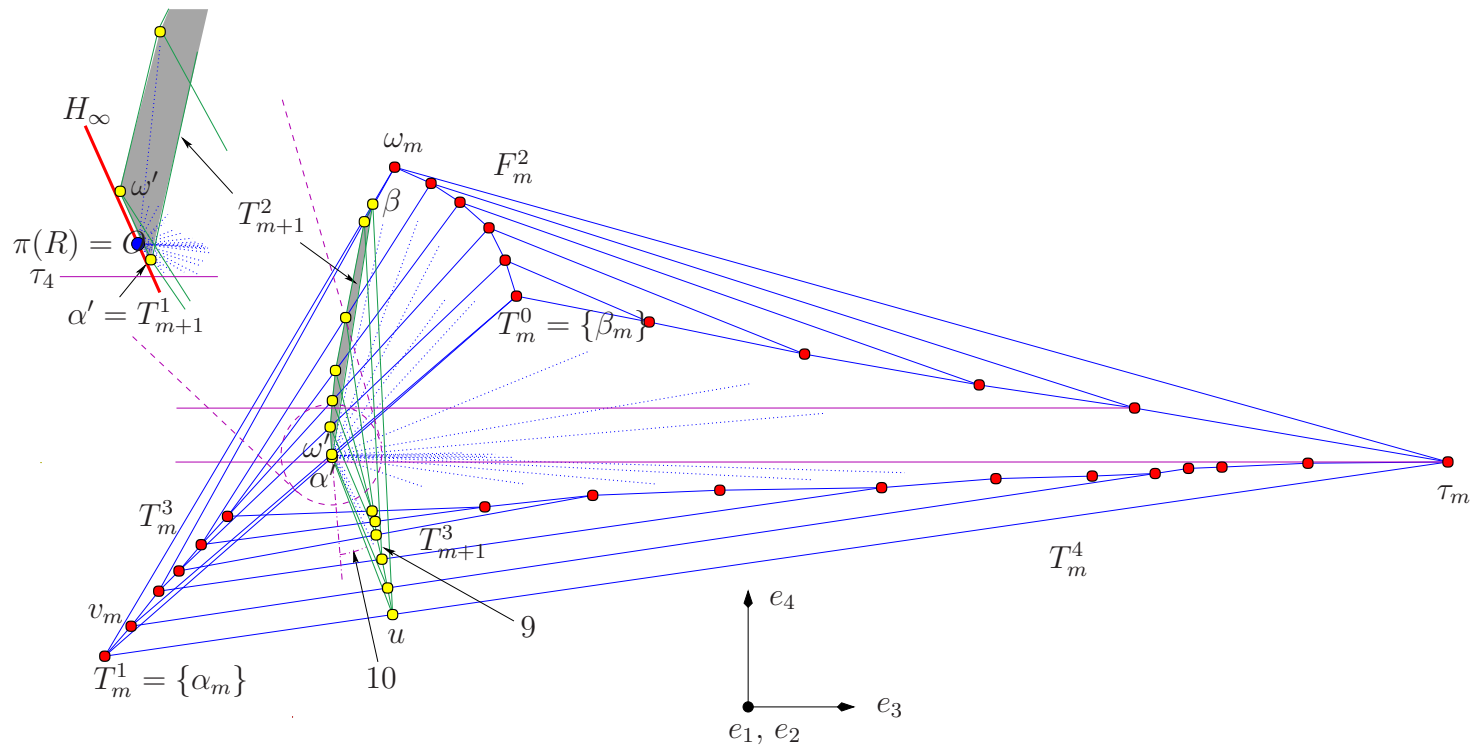


FIGURE 12: *The inductive step:* We show the projection of the polytope Q_4 to the $\langle 3, 4 \rangle$ -plane, and the vertices obtained by intersecting Q_4 with H_5 . The arrows next to the labels 9 and 10 point to the lines about whose slope the corresponding condition in Lemma 5.7 makes an assertion. The line through O is the projection of the 3-plane H_∞ . A sweep around O encounters all vertices of $Q_m \cap H_{m+1}$ in the correct order π_m prescribed by $\tilde{\pi}_{m+1}$.

6. ACKNOWLEDGEMENTS

It is a pleasure to thank Günter M. Ziegler for suggesting this problem, and Volker Kaibel for his careful reading of an earlier version of the paper.

REFERENCES

- [1] DAVID W. BARNETTE, *A family of neighborly polytopes*, *Isr. J. Math.*, **39** (1981), 127–140.
- [2] FRED HOLT and VICTOR KLEE, *A proof of the strict monotone 4-step conjecture*, *Contemp. Math.*, **223** (1999), 201–216.
- [3] MICHAEL JOSWIG, VOLKER KAIBEL, and FRIEDERIKE KÖRNER, *On the k -systems of a simple polytope*, *Isr. J. Math.*, **129** (2002), 109–117.
- [4] VICTOR KLEE, *Heights of convex polytopes*, *J. Math. Anal. Appl.*, **11** (1965), 176–190.
- [5] PETER MCMULLEN, *The numbers of faces of simplicial polytopes*, *Isr. J. Math.*, **9** (1971), 559–570.
- [6] THEODORE S. MOTZKIN, *Comonotone curves and polyhedra*, Abstract, *Bulletin Amer. Math. Soc.*, **63** (1957), 35.
- [7] JULIAN PFEIFLE and GÜNTER M. ZIEGLER, *On the monotone upper bound problem*, *Experimental Math.*, (2004), to appear.
- [8] IDO SHEMER, *Neighborly polytopes*, *Isr. J. Math.*, **43** (1982), 291–314.
- [9] GÜNTER M. ZIEGLER, *Lectures on Polytopes*, Graduate Texts in Mathematics **152**, Springer, New York, 1995. Revised edition 1998.

INSTITUT DE MATEMÀTICA, UNIVERSITAT DE BARCELONA, GRAN VIA DE LES CORTS CATALANES
585, E-08007 BARCELONA, SPAIN

E-mail address: julian@imub.ub.es